TRANSACTIONS ON EMERGING TELECOMMUNICATIONS TECHNOLOGIES
Trans. Emerging Tel. Tech. (2014)
Published online in Wiley Online Library (wileyonlinelibrary.com). DOI: 10.1002/ett.2808

SPECIAL ISSUE PAPER

Performance analysis of TCP over visible light communication networks with ARQ-SR protocol

Vuong V. Mai, Ngoc-Anh Tran, Truong C. Thang and Anh T. Pham*

The Computer Communications Lab., University of Aizu, Japan

ABSTRACT

This paper theoretically studies the performance of transmission control protocol (TCP) over visible light communications (VLC) networks when the automatic-repeat request, selective repeat (ARQ-SR) protocol is employed in the link layer. We analytically derive TCP throughput considering the impact of ARQ-SR parameters and different VLC physical factors, including inter-symbol interference (ISI), signal reflection and light power distribution. Numerical results show that TCP throughput is strongly dependent on the location of VLC user due to impacts of ISI and signal reflection. It is also seen that the use of ARQ-SR could significantly improve both the maximum value and the distribution of TCP throughput in the VLC network. Especially, with a proper selection of the number of re-transmissions by the ARQ-SR protocol, the dependence of TCP throughput on user location caused by ISI, light signal reflection and distribution could be effectively remedied. Copyright © 2014 John Wiley & Sons, Ltd.

***Correspondence**

A. T. Pham, The Computer Communications Lab., University of Aizu, Ikki-machi, Aizuwakamatsu, Fukushima, Japan.
E-mail: pham@u-aizu.ac.jp

Received 15 October 2013; Revised 12 December 2013; Accepted 20 January 2014

1. INTRODUCTION

Light-emitting diode (LED) has been recently considered as the most effective lighting technology due to its many advantages such as high brightness, long life, energy efficiency, durability and affordable cost [1]. More importantly, besides the illumination purpose, LEDs, at the same time, can be used as a transmission medium for high-speed data communications [2, 3]. Such technology is referred to as visible light communications (VLC) and it is being considered as an alternative solution for indoor broadband communications.

Visible light communications technology offers a number of important benefits, including the use of unregulated huge bandwidth, licence-free operation, and possibly low cost [4]. There are nevertheless a number of challenging issues in practical deployments due to the unique characteristics of the VLC physical channel. Over the past decade, there have been many studies dedicated to channel modelling, performance analysis and solution for the performance improvement of VLC systems. For instance, fluctuations of the brightness of light (i.e. the flickering) when transferring data may be harmful to human eyes [5]. Also, dimming control is required to maintain communications while a user arbitrarily dims light source [6]. Caused by object movements, such as people or paper, temporary blocking may happen in VLC links [7]. Additionally, the presence of inter-symbol interference (ISI), reflection (by walls) and non-uniform of light power distribution corresponds to an intentional increase of the link loss [8, 9]. So far, these issues have been considered in a wide variety of VLC studies. Completed in September 2011, the Institute of Electrical and Electronics Engineers 802.15.7 standard supports minimising the flickering and achieving dimming control methods [10]. In [11], Kim *et al*. proposed a resource allocation protocol for solving the problem of frequent blocking in VLC links. Furthermore, the use of forward error correction codes has been introduced to combat link losses [12, 13].

On the other hand, transmission control protocol (TCP) is the most popular transport protocol used by the majority of Internet applications. Because there is a huge amount of Internet traffic access through wireless technologies, issues regarding the behaviour of TCP over wireless networks have been well-studied [14]. Basically, TCP performs well in wired networks where TCP segment losses happen mainly due to congestions. On the other hand, in wireless networks, the losses are mostly caused by lossy links. TCP reacts to these losses by performing congestion control algorithms, which results in the degradation of end-to-end performance, particularly in TCP throughput, which is highly sensitive to losses. This problem has

been addressed in both radio frequency and outdoor optical wireless communications [15–18]. To the best of our knowledge, however, the performance of TCP over VLC network has not been reported in the literature.

In this paper, we therefore present an analytical study on the performance of TCP over VLC networks considering various important VLC physical factors, including ISI, reflection and light power distribution. As confirmed in the numerical results, TCP throughput is critically affected by those factors. To improve the TCP throughput, automatic-repeat request (ARQ), an effective loss-recovery scheme for the data-link layer, is employed [19–21]. Two kinds of ARQ, including ARQ stop-and-wait (ARQ-SW) and ARQ selective repeat (ARQ-SR), are considered. It is seen that while ARQ-SW protocol could improve the throughput distribution, ARQ-SR enhances both the maximum value and the distribution of TCP throughput. Especially, when with a proper selection of the number of re-transmissions by ARQ-SR protocol, the fluctuation of TCP throughput caused by ISI and light signal reflection and distribution could be effectively remedied.

The rest of the paper is organised as follows. System descriptions including the network model and the VLC channel model are detailed in Section 2. In Section 3, TCP throughput is derived by considering TCP-Reno operation, TCP segment-loss probability and average round-trip time (RTT). The numerical analyses and discussions are given in Section 4. Finally, Section 5 concludes the paper.

2. SYSTEM DESCRIPTIONS

2.1. TCP over VLC network model

The network model is described in Figure 1. TCP-Reno [22] is assumed, in which a TCP client located in a VLC indoor local network is connected to a TCP server over the Internet. The network therefore consists of two main parts, the VLC part from the client terminal to the VLC base station and the wired part from the VLC base station to the TCP server.

In the link layer, ARQ-SR protocol is implemented on the VLC network part. In order to focus on the impact of link layer error control, the impact of media access is ignored, that is, we consider only one client and the link layer is therefore assumed to be collision-free. Each TCP segment from upper layer is divided into N_f smaller data units, that is, frames, before being transmitted over the VLC link. In case of ARQ-SW, frames are transmitted one by one. When a frame transmission is successful, the sender, upon receiving an acknowledgment (ACK) from the receiver, will move on to transmit a new frame. It is assumed that an uplink transmitting ACK messages is always available and error free. If frame transmission is failed (either corrupted or lost), the sender will re-transmit that frame. The maximum number of re-transmission is determined by a persistent level, denoted as M. After M rounds of re-transmission, if the frame still cannot be received successfully, the sender will give up and thus the corresponding TCP segment is assumed to be loss. In case of ARQ-SR, sender is allowed to send all frames continuously without waiting for ACK. In addition, ARQ-SR is able to avoid unnecessary re-transmissions as each frame is ACKed separately, and therefore re-transmitted individually when re-transmission is required. We assume that the transmitted data are large enough so that TCP segments are always available at the VLC sender.

Regarding the VLC physical layer, on–off keying modulation scheme is employed thanks to its simplicity and power efficiency [3]. Additionally, the configuration of VLC link is non-directed light-of-sight due to its impor-

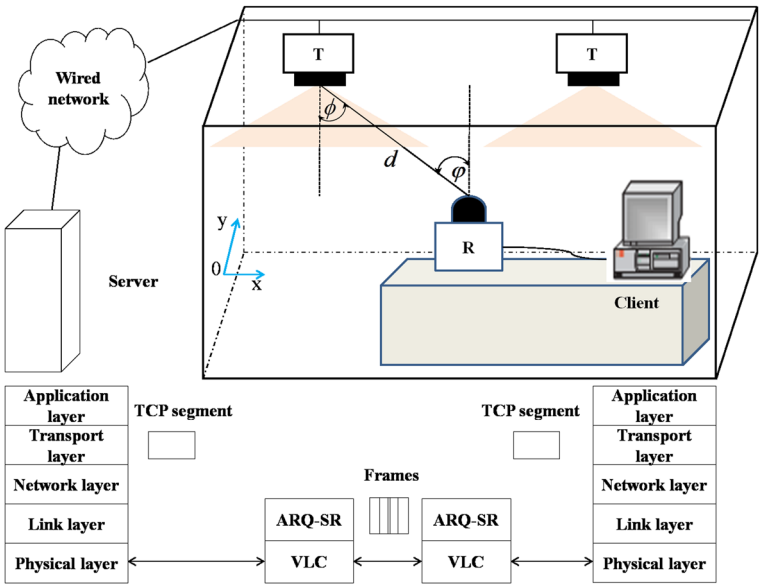

Figure 1. Transmission control protocol connection over visible light communications network model.

tance in general indoor VLC system with dual purpose of illuminance and data communication [10].

2.2. VLC channel model

The visible light channel can be modelled as a linear optical additive white Gaussian noise channel and summarised by

$$y(t) = \gamma x(t) \otimes h(t) + n(t) \tag{1}$$

where $x(t), y(t)$ and $h(t)$ represent the instantaneous transmitted optical power, received signal current and channel impulse response, respectively. $n(t)$ is Gaussian noise, γ is the PD conversion efficiency, and symbol $\otimes$ denotes convolution operator.

The time average transmitted optical power can be derived by the following equation:

$$P_t = \lim_{T\to\infty} \frac{1}{2T} \int_{-T}^{T} x(t)dt \tag{2}$$

The channel direct current(DC) gain is the Fourier transformation of $h(t)$

$$H(0) = \int_{-\infty}^{\infty} h(t)dt \tag{3}$$

and can also be given by [8]

$$H_d(0) = \begin{cases} \frac{(m+1)A}{2\pi d^2} \cos^m(\phi) T_s(\psi) g(\psi) \\ \times \cos(\psi),\ 0 \leqslant \psi \leqslant \Psi_c, \\ 0,\ \psi > \Psi_c \end{cases} \tag{4}$$

where A, d, ϕ and ψ are the physical area of the detector in a photodiode, the distance between the transmitter and the receiver surface, the angle of irradiance with respect to the axis normal to the transmitter surface and the angle of incidence with respect to the axis normal to the receiver surface, respectively. $T_s(\psi)$ is the gain of optical filter, and Ψ_c is the width of the field of vision (FOV) at a receiver. The optical concentrator gain at the receiver, $g(\psi)$, and the order of Lambertian emission, m, are defined by

$$g(\psi) = \begin{cases} \frac{n^2}{\sin^2 \Psi_c},\ 0 \leqslant \psi \leqslant \Psi_c, \\ 0,\ \psi > \Psi_c \end{cases} \tag{5}$$

$$m = \frac{\ln(2)}{\ln(\cos(\Phi_{1/2}))} \tag{6}$$

where n and $\Phi_{1/2}$ are the refractive index and the semi-angle at half illuminance, respectively.

The channel DC gain of the first reflected path is given by [7]

$$\mathrm{d}H_{ref}(0) = \begin{cases} \frac{(m+1)A}{2\pi^2 D_1^2 D_2^2} \rho \mathrm{d}A_{ref} \cos(\alpha) \cos(\beta) \cos^m(\phi_r) \\ \times T_s(\psi_r) g(\psi_r) \cos(\psi_r),\ 0 \leqslant \psi_r \leqslant \Psi_c, \\ 0,\ \psi_r > \Psi_c \end{cases} \tag{7}$$

where D_1 and D_2 are the distance between LED chip to the reflective point and between the reflective point to the receiver surface, respectively. ρ is the reflectance factor, and $\mathrm{d}A_{ref}$ is a reflective area of a small region. ϕ_r is the angle of irradiance to reflective point, and α, β are angles of irradiance and incident to reflective point, respectively.

3. TCP PERFORMANCE ANALYSIS

In this section, the performance of end-to-end TCP connection considering the combined effect of the VLC physical factors and ARQ-SR protocol is theoretically analysed. In particular, the TCP segment-loss probability and the average RTT, which are two key TCP performance indicators, are analytically derived after a brief description of TCP-Reno operation and its throughput evaluation.

3.1. TCP-Reno throughput evaluation

As shown in Figure 2, the behaviour of the TCP-Reno can be described by three key operating phases: slow-start (Ss), congestion avoidance (Ca) and time-out (To). Initially, the congestion window is set to one segment and in Ss phase; if there is no loss event, the congestion window is doubled after each RTT. Its growth continues until it reaches the current Ss threshold ($Ssthresh$); TCP-Reno then switches to the Ca phase. In Ca, if there is no loss, the window size will increase by one segment per RTT. This window size increase remains until either the congestion window reaches the maximum window size (W_{max}), or there is a loss event. If the loss event is a triple-duplicate ACK, TCP-Reno cuts the congestion window size to a half and

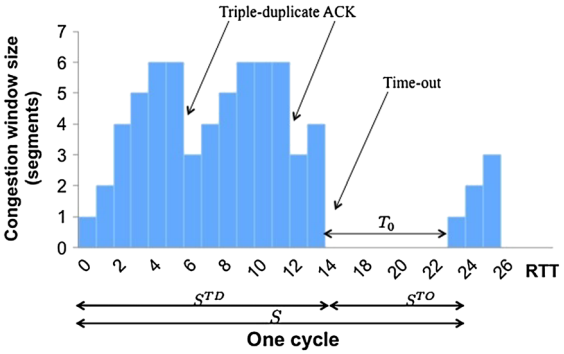

Figure 2. An example of transmission control protocol Reno operation when $W_{max} = 6$.

continues staying in the *Ca* phase. If a *To* occurs, TCP-Reno switches to *To* phase and sets the *Ssthresh* by a half of the current congestion window size. TCP sender will wait for a *To* duration, T_0, before trying to transmit a segment in a new *Ss* phase. More details of TCP-Reno operation can be found in [23].

Because of the nature of congestion control algorithm, there is a change in the congestion window size after each RTT, which results in a fluctuation of the throughput. TCP-Reno throughput estimation can be evaluated using either simulation tools and implementation measurement [24] or theoretical analysis. Regarding the theoretical analysis, M. Mathis *et al.* developed a macroscopic description of TCP-Reno throughput in [25]. However, as this method uses unrealistic assumptions for the sake of simplification (e.g. the values of *Ssthresh* and RTT are constant), its accuracy is limited. A closed-form expression for the TCP-Reno throughput has been derived by using a Markov chain model [26]. However, this method is complicated due to the need of mapping various phase operations of the congestion control algorithms (i.e. *Ss, Ca* and *To*) into the Markov chain.

In this paper, for a balance between simplicity and accuracy, we employ the full-approximated model for TCP throughput [23, 27]. This approximation is based on breaking down time-line operation into cycles. Each cycle (S) includes two periods: (i) the period where all losses are indicated by triple-duplicate ACK (S^{TD}) and (ii) the period where all losses are indicated by *To* (S^{TO}). By defining K as the total number of segments sent during interval S, the average TCP-Reno throughput is given by

$$\begin{aligned}\Im_{Re} &= \frac{E[K]}{E[S]} \\ &= \frac{E\left[K^{TD}\right] + E\left[K^{TO}\right]}{E\left[S^{TD}\right] + E\left[S^{TO}\right]}\end{aligned} \tag{8}$$

where

$$\begin{aligned}E\left[K^{TD}\right] &= E\left[n^{TD}\right]E\left[k^{TD}\right], \\ E\left[K^{TO}\right] &= E\left[n^{TO}\right]E\left[k^{TO}\right], \\ E\left[S^{TD}\right] &= E\left[n^{TD}\right]E\left[s^{TD}\right], \\ E\left[S^{TO}\right] &= E\left[n^{TO}\right]E\left[s^{TO}\right]\end{aligned} \tag{9}$$

Here, $E\left[n^{TD}\right]$ and $E\left[n^{TO}\right]$ are the average number of triple-duplicate ACKs and time-outs happening in a cycle; $E\left[k^{TD}\right]$ and $E\left[k^{TO}\right]$ are the average number of segments transmitted in a triple-duplicate ACKs period and a *To* period; $E\left[s^{TD}\right]$ and $E\left[s^{TO}\right]$ are the average length of a triple-duplicate ACK period and a *To* period. Basically, those parameters are functions of the TCP segment-loss probability ($\mathbb{P}$), the average round-trip time (E[RTT]) and the initial time-out duration (T_0). By applying derivations of the parameters in [23], we obtain the approximation of TCP-Reno as

$$\Im_{Re} \approx \frac{1}{\mathrm{E[RTT]}\sqrt{\frac{4\mathbb{P}}{3}} + T_0 \min\left(1, 3\sqrt{\frac{6\mathbb{P}}{8}}\right)\mathbb{P}(1+32\mathbb{P}^2)} \tag{10}$$

Note that, we do not consider any limitation on the congestion window size in the aforementioned derivation. As the congestion window size remains unchanged when it reaches the maximum window size (W_{max}), the throughput in this case is given by

$$\Im_{Re} = \frac{W_{max}}{\mathrm{E[RTT]}} \tag{11}$$

Finally, after combining Equations (10) and (11), we have the full approximation of $\Im_{Re}$ as follows [27]:

$$\Im_{Re} \approx \min\left(\frac{W_{max}}{\mathrm{E[RTT]}}, \frac{1}{\mathrm{E[RTT]}\sqrt{\frac{4\mathbb{P}}{3}} + T_0 \min\left(1, 3\sqrt{\frac{6\mathbb{P}}{8}}\right)\mathbb{P}(1+32\mathbb{P}^2)}\right) \tag{12}$$

As given in Equation (12), to calculate TCP throughput, two key parameters, including TCP segment-loss probability ($\mathbb{P}$) and the average round-trip time (E[RTT]), need to be considered.

3.2. TCP segment-loss probability

Let P_{VLC} and P_{wire} denote the segment-loss probabilities in the VLC link and wired network, respectively, the TCP segment-loss probability can be expressed as

$$\mathbb{P} = 1 - (1 - P_{VLC})(1 - P_{wire}) \tag{13}$$

The TCP segment-loss probability on the VLC link under the ARQ-SR protocol can be written as

$$P_{VLC} = 1 - \left(1 - P_f^{M+1}\right)^{N_f} \tag{14}$$

in which P_f is the frame-error probability on the VLC link and given by

$$P_f = 1 - (1 - P_e)^{L_f} \tag{15}$$

where L_f is the frame length and P_e is bit-error probability.

The bit-error rate P_e, when on–off keying is employed, can be expressed in terms of electrical signal-to-noise ratio as

$$P_e = \mathrm{Q}\left(\sqrt{\mathrm{SNR}}\right) \tag{16}$$

where $Q(y) = \frac{1}{\sqrt{2\pi}} \int_y^{\infty} \exp\left(-\frac{y^2}{2}\right) dy$ is the Gaussian Q-function. The signal-to-noise ratio can be expressed in terms of the photodetector responsivity, γ, the received optical power and noise variances as

$$\mathrm{SNR} = \frac{(\gamma P_r)^2}{\sigma_{\mathrm{shot}}^2 + \sigma_{\mathrm{thermal}}^2 + P_{ISI}} \tag{17}$$

The received optical power, P_r, is the total power received from the directed path and first reflected path, which is derived as

$$P_r = \sum^{LEDs} \left\{ P_t H_d(0) + \int_{walls} P_t \mathrm{d}H_{ref}(0) \right\} \tag{18}$$

where P_t is the average transmitted optical power, which is assumed to be the same for all LEDs. $H_d(0)$ and $H_{ref}(0)$ are given in Section 2.2, that is, Equations (3) and (7), respectively.

Moreover, in case of indoor VLC channel, the noise in VLC receiver is similar to the traditional optical receiver, which are thermal noise from load resistor, shot noise in photodiode and excess noise from the amplifier [9]. The main noise component is other illumination light, which is the major reason of ISI phenomenal. In multi-path case with ISI, the desired received power and ISI power are given by [8]

$$P_{rSignal} = \int_0^T \left(\sum_{i=1}^{LEDs} h_i(t) \otimes x(t) \right) dt \tag{19}$$

$$P_{ISI} = \int_T^{\infty} \left(\sum_{i=1}^{LEDs} h_i(t) \otimes x(t) \right) dt \tag{20}$$

Here, $h_i(t)$ is the impulse response of the channel from i-th LED to the receiver. Two remaining noise variances in Equation (17) are thus given by

$$\sigma_{\mathrm{shot}}^2 = 2q\gamma(P_{rSignal} + P_{ISI})B + 2qI_B I_2 B \tag{21}$$

$$\sigma_{\mathrm{thermal}}^2 = \frac{8\pi\kappa T_k}{G_{ol}} C_{pd} A I_2 B^2 + \\ + \frac{16\pi^2 \kappa \Gamma T_k}{g_m} C_{pd}^2 A_{PD}^2 I_3 B^3 \tag{22}$$

The first term represents shot-noise variance, in which q, I_2 and I_B are the electronic charge, the noise-bandwidth factor and the background current measured by using the direct sun light, respectively. The equivalent noise bandwidth $B = R_b$ is set, with R_b is the VLC channel data rate. The second term expresses the thermal noise variance, where κ is the Boltzmann's constant, T_k is the absolute temperature, G_{ol} is the open-loop voltage gain, C_{pd} is the fixed capacitance of photodetector per unit area, Γ is the field effect transistors channel noise factor, g_m is the field effect transistors transconductance and I_3 is the noise-bandwidth factor.

3.3. Average round-trip time

The average RTT can be defined as the average of time period from the time when TCP source transmits a segment to the time when the corresponding ACK comes back to the source. Though when transmitting a TCP segment in the VLC part, the segment is divided into N_f frames, the average time consumptions caused by re-transmission processes for a segment and a frame are approximately equal. This is due to ARQ-SR's ability of transmitting frames continuously. Therefore, E[RTT] is approximated as follows:

$$\mathrm{E[RTT]} \approx 2 \times T_{wire} + (L_f/R_b + T_{CRC})(\overline{M} + 1) \tag{23}$$

where T_{wire} is one-way transmission time in the wired part. T_{CRC} is the error detection time that data-link layer spends on checking the cyclic redundancy check field and recognising a corrupted frame. L_f/R_b is the time required for transmitting one frame. $\overline{M}$ is the average number of re-transmission for one frame.

Next, let us denote β as the number of re-transmission times for transmitting successfully a frame. Obviously, β is an i.i.d. geometric random variable whose probability density function is given as

$$\begin{cases} P\{\beta = i\} = \frac{P_f^i(1-P_f)}{1-P_f^{M+1}}, 0 \leqslant i \leqslant M, \\ P\{\beta = i\} = 0, \text{otherwise} \end{cases} \tag{24}$$

Here, M is the persistent level, P_f is the frame-error probability given in Equation (15); $\overline{M}$ is exactly the expectation of β, and therefore, can be given as

$$\begin{aligned} \overline{M} &= \sum_{i=0}^{\infty} iP\{\beta = i\} \\ &= \sum_{i=0}^{\infty} i \frac{P_f^i(1-P_f)}{1-P_f^{M+1}} = \frac{P_f(1-P_f)}{1-P_f^{M+1}} \sum_{i=1}^{M} iP_f^{i-1} \\ &= \frac{P_f(1-P_f)}{1-P_f^{M+1}} \frac{\partial}{\partial P_f} \left(\frac{1-P_f^{M+1}}{1-P_f} \right) \\ &= \frac{P_f(1-P_f)}{1-P_f^{M+1}} \frac{(M+1)P_f^M(P_f-1) + \left(1-P_f^{M+1}\right)}{(1-P_f)^2} \\ &= \frac{P_f}{1-P_f} - \frac{(M+1)P_f^{M+1}}{1-P_f^{M+1}} \end{aligned} \tag{25}$$

Table I. System parameters.

Series name	Series symbol	Series value
VLC channel data rate	R_b	100 Mb/s
Maximum congestion window size	W_{max}	16
Num. acknowledged segments/ ACK	b	2
Initial time-out	T_0	5 s
TCP segment size	L_{TCP}	1360 Bytes
Frame size	L_f	268 Bytes
Wired part transmission time	T_{wire}	60 ms
CRC checking time	T_{CRC}	10 ms
Segment loss of the wired network	P_{wire}	0

VLC, visible light communications; ACK, acknowledgment; TCP, transmission control protocol; CRC, cyclic redundancy check.

4. NUMERICAL RESULTS AND DISCUSSIONS

In this section, using the previously derived formulations, that is, Equations (12), (13) and (23), we analyse the TCP performance over VLC networks in cases of with and without applying ARQ scheme in the link layer. The system parameters related to TCP and the link layer are shown in Table I. Regarding the VLC physical layer, the room size is $5 \times 5 \times 3\,m^3$, and the number of LEDs arrays is 4. Each LED array has 3600 (60×60) LEDs with transmitted optical power by individual LED is 20 mW, the space between LEDs is 1 cm. The semi-angle at half power of an LED is 60°. LED arrays are 2.5 m high from the floor, and their positions are (1.25,1.25), (1.25,3.75), (3.75,1.25) and (3.75, 3.75). The user terminal placed on the table with the height of 0.85 m and the receiver has a $FOV = 65°$. Other parameters are set as follows: $T_s(\psi) = 1$, $\phi_c = 1$, $A_{PD} = 1$ cm^2, $n = 1.5$, and $\phi_c = 70°$, $I_2 = 0.562$, $I_B = 5100\,\mu$A, $T_k = 295$ K, $G_{ol} = 10$, $C_{pd} = 1.6$ pF/cm^2, $\Gamma = 1.5$, $g_m = 30$ mS, and $I_3 = 0.0868$.

4.1. TCP throughput over VLC networks without ARQ

First, Figures 3 and 4 show the TCP throughput distributions without ARQ for two cases: (i) only effect of light power distribution is considered, both ISI and relocation are ignored, and (ii) considering all effects. Using these figures, the impact of important VLC physical factors on TCP throughput can be comprehensively analysed. It is seen that there exists a non-uniform throughput distribution. The present of this phenomenon is due to the fact that there are some areas, corresponding to positions under four LED arrays or their overlap light power distribution areas, that receive higher power from transmitters, whereas others receive much less power. As a result, in those areas that receive higher power, TCP throughput reaches the maximum value of 180 kB/s; at the same time, the TCP throughput is about 110 kB/s for other areas.

All impacts of light power distribution, ISI and reflection are considered in Figure 4. As is evident, the phenomenon of TCP throughput distribution changes drastically. While the maximum throughput areas tend to relocate into positions near wall surfaces, the value of minimum throughput is dropped significantly (from 110 kB/s as in Figure 3 to about 10 kB/s). This is due to the fact that while the reflection plays a role in enhancing received signal power, especially in locations near wall surfaces, it has a large influence on increasing ISI, which lead to a decrease of TCP performance.

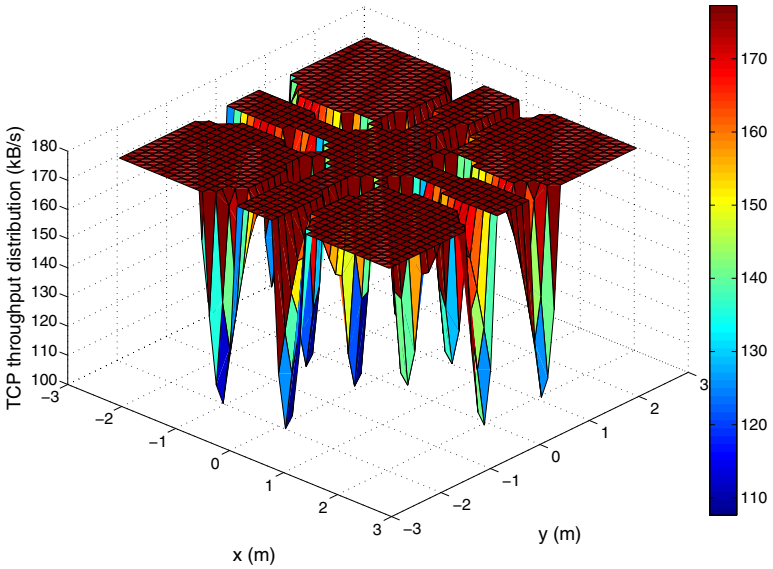

Figure 3. TCP throughput distribution without ARQ, both ISI and reflection are ignored.

DOI: 10.1002/ett

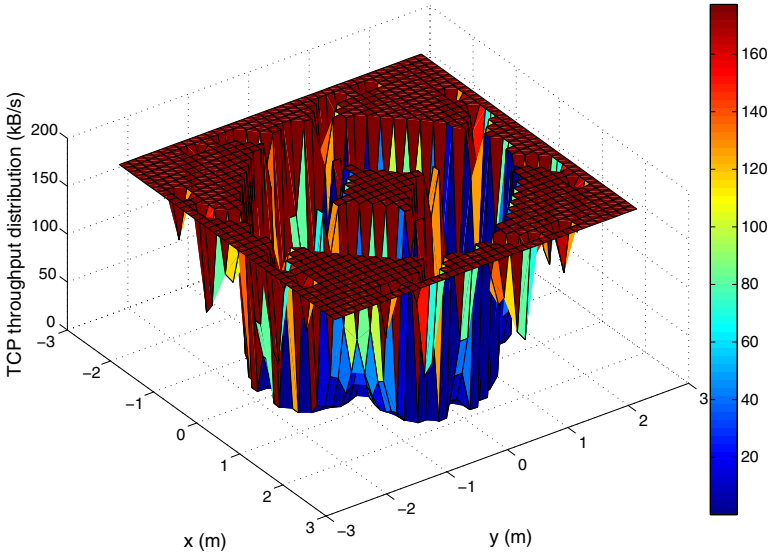

Figure 4. TCP throughput distribution without ARQ, impact of both ISI and reflection is included.

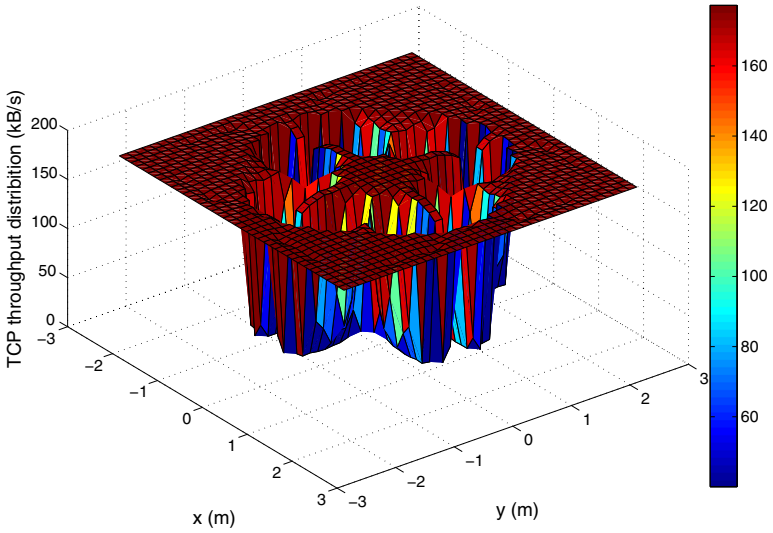

Figure 5. TCP throughput distribution with ARQ-SW ($M = 1$) and considering both ISI and reflection.

4.2. TCP throughput over VLC networks with ARQ

Now, we highlight the advantage of ARQ schemes to improve the TCP throughput. Two types of ARQ are considered, ARQ-SW and ARQ-SR. Note that, while the TCP segment-loss probabilities, $\mathbb{P}$, are the same in both cases of ARQ-SW and ARQ-SR, E[RTT] corresponding ARQ-SW is different from the derivation in Equation (23). As in the operation of ARQ-SW, the next frame is transmitted after the sender receives ACK of the previous frame, E[RTT] is given as $\text{E[RTT]} \approx 2 \times T_{wire} + (L_f/B + T_{CRC})(\overline{M} + 1)N_f$ [28].

In Figure 5, it is seen that, when ARQ-SW is employed, an improvement in TCP throughput distribution can be observed. Furthermore, the ARQ-SW protocol also enhances the minimum value of throughput. More specifically, even $M = 1$ is employed, the minimum throughput of TCP reaches 50 kB/s. However, the maximum value of throughput stays unchanged at 180 kB/s.

Figure 6 shows a result corresponding to the case when ARQ-SR protocol is employed. Because of the ability of transmitting frames continuously without waiting for the ACK, E[RTT] is decreased and thus the TCP throughput is greatly improved when comparing with that of ARQ-SW. As expected, the maximum values of TCP throughput could be improved by approximately 40 kB/s when using ARQ-SR instead of ARQ-SW at the link layer.

Finally, the results of Figures 4, 5 and 6 are confirmed again in Figure 7. Note that this figure have been performed by taking a set of points that satisfy the condition of $x = y$ in the throughput distribution surface. More importantly,

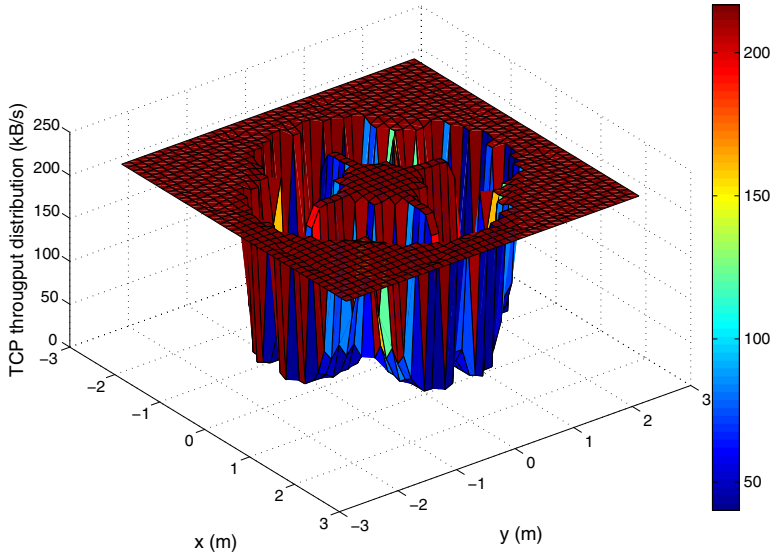

Figure 6. TCP throughput distribution with ARQ-SR ($M = 1$) and considering both ISI and reflection.

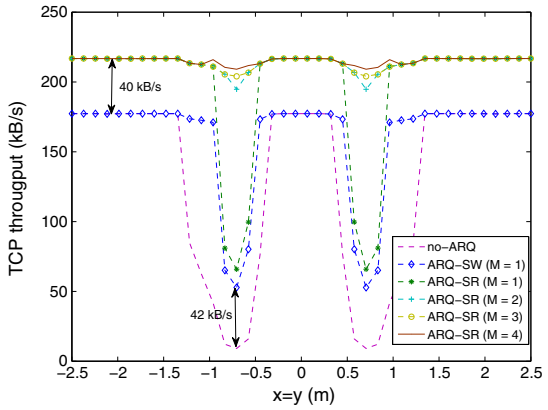

Figure 7. TCP throughput for various values of M and considering both ISI and reflection.

we also compare the performance of the system applying ARQ-SR for different values of the persistent level. It is intuitively clear that the increase in persistent level M could significantly improves TCP throughput distribution. However, a point of interest is that the throughput reaches closely to the maximum level and remains almost unchanged when M is higher than 3. This is because while the use of ARQ-SR decreases the TCP segment-loss probability, it significantly increases the average end-to-end transmission delay caused by the re-transmission processes. It is therefore recommended that $M = 3$ is the optimal value for the analysed system applying ARQ-SR in the link layer of VLC networks.

5. CONCLUSIONS

We have analytically studied the performance of TCP over VLC networks in cases of with and without ARQ scheme in the link layer. Many VLC physical factors including light power distribution, ISI and reflection were taken into consideration in the TCP performance analysis. Also, two types of ARQ scheme, including ARQ-SW and ARQ-SR, were considered. Numerical results showed that the impacts of VLC physical factors on the TCP throughput are severe. However, using ARQ schemes could significantly improve the TCP performance. In addition, the systems employing ARQ-SR offer better performance than that of the ones with ARQ-SW, especially in terms of maximum TCP throughput. In addition, it was found that the selection of persistent level could significantly improve the TCP throughput distribution, and it was recommended that the persistent level $M = 3$ is the optimal value for ARQ-SR in the analysed system.

REFERENCES

1. Stringfellow GB, Craford MG. *High Brightness Light Emitting Diodes*, Vol. 48. Semiconductors and Semimetals Academic Press: London, UK, 1997, 65–95.
2. Grubor J, Randel S, Langer KD, Walewski JW. Broadband information broadcasting using LED-based interior lighting. *Journal of Lightwave Technology* 2008; **26**(24): 3883–3892. DOI: 10.1109/JLT.2008.928525
3. Le Minh H, OBrien D, Faulkner G, Zeng L, Lee K, Jung D, Oh YJ, Won ET. 100-Mb/s NRZ visible light communications using a postequalized white LED. *IEEE Photonics Technology Letters* 2009; **21**(15): 1063–1065. DOI: 10.1109/LPT.2009.2022413
4. Elgala H, Mesleh R, Haas H. Indoor optical wireless communication: potential and state-of-the-art. *IEEE Communications Magazine* 2011; **49**(9): 56–62. DOI: 10.1109/MCOM.2011.6011734

5. Berman SM, Greenhouse DS, Bailey IL, Clear RD, Raasch TW. Human electroretinogram responses to video displays, fluorescent lighting and other high frequency sources. *Optometry and Vision Science* 1991; **68**(8): 645–62.
6. Rajagopal S, Roberts RD, Lim SK. IEEE 802.15.7 visible light communication: modulation schemes and dimming support. *IEEE Communications Magazine* 2012; **50** (3): 72–82. DOI: 10.1109/MCOM.2012.6163585
7. Komine T, Haruyama S, Nakagawa M. A study of shadowing on indoor visible-light wireless communication utilizing plural white LED lightings. *Kluwer Wireless Personal Communications* 2005; **34**(1): 211–225. DOI: 10.1109/ISWCS.2004.1407204
8. Komine T, Nakagawa M. Fundamental analysis for visible-light communication system using LED lights. *IEEE Transactions on Consumer Electronics* 2004; **50**(1): 100–107. DOI: 10.1109/TCE.2004.1277847
9. Lee K, Park H, Barry JR. Indoor channel characteristics for visible light communications. *IEEE Communications Letters* 2011; **15**(2): 217–219. DOI: 10.1109/LCOMM.2011.010411.101945
10. IEEE Standard for Local and Metropolitan Area Networks. Part 15.7: Short-range wireless optical communication using visible light, IEEE Std 802.15.7, 2011, 1–309.
11. Kim WC, Bae CS, Jeon SY, Pyun SY, Cho DH. Efficient resource allocation for rapid link recovery and visibility in visible-light local area networks. *IEEE Transactions on Consumer Electronics* 2010; **56**(2): 524–531. DOI: 10.1109/TCE.2010.5505965
12. Kim S, Jung SY. Novel FEC coding scheme for dimmable visible light communication based on the modified reed muller codes. *IEEE Photonics Technology Letters* 2011; **23**(20): 1514–1516. DOI: 10.1109/LPT.2012.2199104
13. Lee SH, Kwon JK. Turbo code-based error correction scheme for dimmable visible light communication systems. *IEEE Photonics Technology Letters* 2012; **24**(17): 1463–1465. DOI: 10.1109/LPT.2012.2199104
14. Huston G. TCP in a wireless world. *IEEE Internet Computing* 2001; **5**(2): 82–84. DOI: 10.1109/4236.914651
15. Lee J, Lee HW, Yi Y, Chong S. Improving TCP performance over optimal CSMA in wireless multi-hop networks. *IEEE Communications Letters* 2012; **16**(9): 1388–1391. DOI: 10.1109/LCOMM.2012.071612.120157
16. Liu H, Gu Y. TCP with hop-oriented network coding in multi-radio multi-channel wireless mesh networks. *IET Networks* 2012; **1**(3): 171–180. DOI: 10.1049/iet-net.2012.0048
17. Silva Goncalves RF, Delisandra Feltrim V, Fondazzi Martimiano LA. TCP-UEM: detecting link failure by keeping end-to-end semantics. *IEEE Latin America Transactions* 2013; **11**(3): 975–982. DOI: 10.1109/TLA.2013.6568842
18. Mai VV, Thang TC, Pham AT. On the performance of TCP over free-space optical atmospheric turbulence channels. *IEEE/OSA Journal of Optical Communications and Networking* 2013; **5**(11): 1168–1177. DOI: 10.1364/JOCN.5.001168
19. http://www.ieee802.org/15/ [1 October 2013].
20. Kim JG, Krunz MM. Delay analysis of selective repeat ARQ for a Markovian source over a wireless channel. *IEEE Transactions on Vehicular Technology* 2000; **49**(5): 1968–1981. DOI: 10.1109/25.892598
21. Hayashida Y, Maeda A, Sugimachi N, Fujii S. Performance analysis of go-back-N ARQ scheme with selective repeat in intra-block. *IEEE Transactions on Communications* 2002; **50**(3): 391–395. DOI: 10.1109/26.990900
22. Khan MNI, Ahmed R, Aziz MT. A survey of TCP Reno, new Reno and sack over mobile ad-hoc network. *International Journal of Distributed and Parallel Systems* 2012; **3**(1): 49–63. DOI: 10.5121/ijdps.2012.3104
23. Padhye J, Firoiu V, Towsley DF, Kurose JF. Modeling TCP Reno performance: a simple model and its empirical validation. *IEEE/ACM Transactions on Networking* 2000; **8**(2): 133–145. DOI: 10.1109/90.842137
24. Li H, Siu KY, Tzeng HY, Ikeda C, Suzuki H. A simulation study of TCP performance in ATM networks with ABR and UBR services. *IEEE INFOCOM* 1996; **3**: 1269–1276. DOI: 10.1109/INFCOM.1996.493073
25. Mathis M, Semske J, Mahdavi J, Ott T. The macroscopic behavior of the TCP congestion avoidance algorithm. *Computer Communication Review* 1997; **27**(3): 67–82.
26. Casetti C, Meo M. A new approach to model the stationary behavior of TCP connections. *Proceedings of IEEE INFOCOM* 2000; **1**: 367–375. DOI: 10.1109/INFCOM.2000.832207
27. Luo C, Yu FR, Ji H, Leung VCM. Cross-layer design for TCP performance improvement in cognitive radio networks. *IEEE Transactions on Vehicular Technology* 2010; **59**(5): 2485–2495. DOI: 10.1109/TVT.2010.2041802
28. Di Marco P, Rinaldi C, Santucci F, Johansson KH, Moller N. Performance analysis and optimization of TCP over adaptive wireless links. In *IEEE 17th International Symposium on Personal, Indoor and Mobile Radio Communications*, Helsiniki, Finland, 2006; 1–6, DOI: 10.1109/PIMRC.2006.254091.